J. Min. Metall. Sect. B-Metall. 47 (2) B (2011) 211 - 218

Journal of Mining and Metallurgy

AVRAMI BEHAVIOR OF MAGNETITE NANOPARTICLES FORMATION IN CO-PRECIPITATION PROCESS

R. Ahmadi[#], H.R. Madaah Hosseini and and A. Masoudi

Department of Materials Science and Engineering,
Sharif University of Technology, P.O. Box 1458889694, Tehran, Iran

(Received 30 March 2011; accepted 25 April 2011)

Abstract

In this work, magnetite nanoparticles (mean particle size about 20 nm) were synthesized via co-precipitation method. In order to investigate the kinetics of nanoparticle formation, variation in the amount of reactants within the process was measured using pH-meter and atomic absorption spectroscopy (AAS) instruments. Results show that nanoparticle formation behavior can be described by Avrami equations. Transmission electron microscopy (TEM) and X-ray diffraction (XRD) were performed to study the chemical and morphological characterization of nanoparticles. Some simplifying assumptions were employed for estimating the nucleation and growth rate of magnetite nanoparticles.

Key words: Avrami; Magnetite; Nanoparticles; Co-precipitation.

1. Introduction

Nanometric particles show magnetic, mechanical and biological properties different from larger ones due to their smaller size and larger surface area [1-4]. Magnetite nanoparticles in the form of stable ferrofluids have potential applications in drug delivery, cancer therapy, magnetic resonance imaging (MRI) contrast enhancement agent, etc [5-8]. The ability to control and predict the particles morphology and size in synthesis processes, provides good conditions for optimizing ferrofluids suitable for each of these applications. For example, in the case of drug delivery,

[#] *Corresponding author: reahmady@yahoo.com*

DOI:10.2298/JMMB1103300010A

magnetite nanoparticles, ranging from 20-40 nm, mostly accumulate in lymph nodes, so are suitable for imaging or drug delivery for these tissues, while target organs for larger particles, in the range of 80-150 nm, are liver and spleen [4]. Among various processes for nanoparticles synthesis [3, 9-11], co-precipitation method is very prevalent due to its advantages, however, controlling of particles size and shape in this process is difficult due to complicated nature of mechanism and kinetics of such process. General reaction for magnetite formation from initial salt solutions and alkaline source may be shown in the simplified form of [12]:

$$2Fe^{3+} + Fe^{2+} + 8OH^- \rightarrow Fe_3O_4 + 4H_2O \quad ...(1)$$

Given the certain stoichiometry of reaction, rate of Fe_3O_4 particles formation can be studied through the measurement of one or more reactants and products concentration within the process.

In many of solid-solid [13, 14] and liquid-solid [15] phase transformations, rate of reaction or transformation have an Avrami behavior with the general form of [13]:

$$f(t) = 1 - \exp(-kt^n) \quad ...(2)$$

in which t is time, $f(t)$ is fraction of transformation progression and k and n are two constants which are dependent to experimental conditions such as pH and temperature, reactants and products concentrations, etc. In the case of spherical growth, by some simplifying assumptions, it can be written [13]:

$$k = \frac{4}{3}\pi N v^3 \quad ...(3)$$

in which N and v are nucleation points and growth rates, respectively n is around 3 in this case. Time in which $f(t)=0.5$, $t_{0.5}$, can be calculated using equation (4):

$$t_{0.5} = \frac{1}{v}\left(\frac{0.17}{N}\right)^{\frac{1}{3}} \quad ...(4)$$

v as a function of temperature can be written in the form of an Arrhenius equation:

$$v = B\exp\left(-\frac{Q_E}{RT}\right) \quad ...(5)$$

in which B is a constant and Q_E is driving force for precipitation transformation. Equation (6) can be derived from equations (4) and (5) using some simplifying assumptions as below:

$$\frac{\partial(\ln t_{0.5})}{\partial(\frac{1}{T})} = \frac{Q_E}{R} \quad ...(6)$$

Thus, transformation driving force can be determined from $\ln t_{0.5} - \frac{1}{T}$ diagram slope.

Up to now, equation (2) has been proposed for evaluation of some solid state transformations such as pearlitic or precipitation transformations [13]. In this investigation, variation of pH and Fe concentration of solution phase was detected and used for kinetic study of magnetite nanoparticles formation. Until now, authors have proposed some mechanisms for magnetite formation according to general reaction (1) [16, 17] which indicate formation of some intermediate phases such as $Fe(OH)_2$ and $Fe(OH)_3$ before magnetite formation. In this work, these stages are not considered and only kinetics of the final solid phase formation, magnetite, is investigated according to equation (1). First, coincidence of experimental results with equation (2) was investigated. Then, k and n coefficients were calculated under experimental conditions of process and nucleation and growth rate of magnetite nanoparticles formation were evaluated.

XRD, TEM, and AAS experiments were used to investigate chemical and morphological characterization of synthesized ferrofluids. Finally, an Avrami behavior and related kinetic equations were proposed for Fe_3O_4 nanoparticles formation by co-precipitation process. This equation can be used for controlling and predicting the final size and shape of produced nanoparticles in similar co-precipitation processes.

2. Experimental Procedure

2. 1. Sample preparation

All chemical reagents in this study were of analytical grade and used as received without further purification. The typical procedure for synthesizing magnetite nanoparticles is as follows; first pure argon was blown to distilled water to remove oxygen from the solution. After that 0.5 mmol (0.1 g) $FeCl_2.4H_2O$ and 1 mmol (0.27 g) $FeCl_3.6H_2O$ were added to the solution. The mixture was then stirred for 10 min at room temperature and then added suddenly to sodium hydroxide (NaOH) solution, and finally followed by stirring and applying pure argon. pH variation of mixture with time was detected and recorded as a sign of reaction progress. During the reaction, 5 cc liquid samples were taken from reaction container in various time intervals to determine the Fe concentration of solution via AAS analysis. When pH reached a constant amount, stirring was continued for 10 min and then dark precipitates were extracted from container using a strong Sm-Co magnet. These powders were centrifuged for 15 min at 15000 rpm and then washed three times with hexane. Dried powders were prepared for XRD and TEM characterization. To investigate the effect of temperature and initial pH on the rate of particles formation, synthesis experiments were performed in 25, 40, 60 and 70 ^oC, and initial pH of 11.92, 12.1 and 12.3.

2. 2. Apparatus and characterizations

XRD was performed by a Siemens D5000 X-ray diffractometer using graphite-monochromatized high-intensity Cu-K_α radiation (λ= 1.5406 °A). A ZEISS EM-10C TEM was used to determine the average particle size and morphology of the powders on an accelerating voltage of 100 kV. AAS was employed for determination of changes in Fe concentration of solution. Metroem pH meter was used to evaluate pH variation of solution phase with time.

3. Results and discussion

3. 1. XRD results

XRD pattern of dried powder produced at 25^oC is shown in Fig. 1. Six characteristic peaks for Fe_3O_4 nanoparticles (2θ = 30.16˚, 35.48˚, 43.13˚, 53.49˚, 56.91˚ and 62.71˚) marked by their indices (220), (311), (400), (422), (511) and (440) respectively, were recognized for this sample. The mean crystallite size of particles was calculated using the Scherrer's equation, $D = \frac{K\lambda}{\beta \cos\theta}$, on the reflections with (311), (400) and (440), where K is constant, λ is the wavelength of used X-ray, β is the corrected

full width at half maximum (FWHM) and θ is the Bragg's angle. Due to the ceramic nature of Fe_3O_4 nanoparticles, assumption of crystallite size of these nanoparticles as particle size is logical. The mean size of nanoparticles was calculated as about 20 nm for this sample which is in good agreement with TEM observation of the Fe_3O_4 nanoparticles.

3.2. pH measurment, AAS and TEM results

Variation of pH and Fe concentration of solution phase with time for tests carried out at 25, 40, 55 and 70 ^oC are graphically shown in Fig. 2. These data are determined from at least 3 measurements. According to reaction (1) these amounts would decrease with reaction progression. On the other hand, if stoichiometry of reaction (1) satisfies thoroughly, *f(t)* within the process can be calculated through dividing the changes in hydroxide or iron ion concentration at any time to total variation of these amounts. With this approach, *f(t)* can be written as:

$$f(t) = \frac{10^{-pOH_0} - 10^{-pOH_t}}{10^{-pOH_0} - 10^{-pOH_\infty}} \quad ...(7)$$

in which, 10^{-pOH_0}, 10^{-pOH_∞} and 10^{-pOH_t} are OH^- molar concentration of solution phase in start, end and "t" sec after beginning of synthesis process, respectively. Similar equation can be written with respect to iron ions measured by AAS. Accordingly, *f(t)* –ln *t* curves are drawn in Fig. 3 using experimental data of Fig.2.

In order to investigate the accordance of these results with that of Avrami behavior, the following equation, which can be derived from equation (2), can be used in that if $\ln[-\ln(1-f(t))]$ *versus ln t* is a linear or semi-linear plot, experimental results will be coincident with equation (2):

$$\ln[-\ln(1-f(t))] = \ln k + n \ln t \quad ...(8)$$

In this condition, *n* and *k* can be evaluated from slope and intercept with vertical axis,

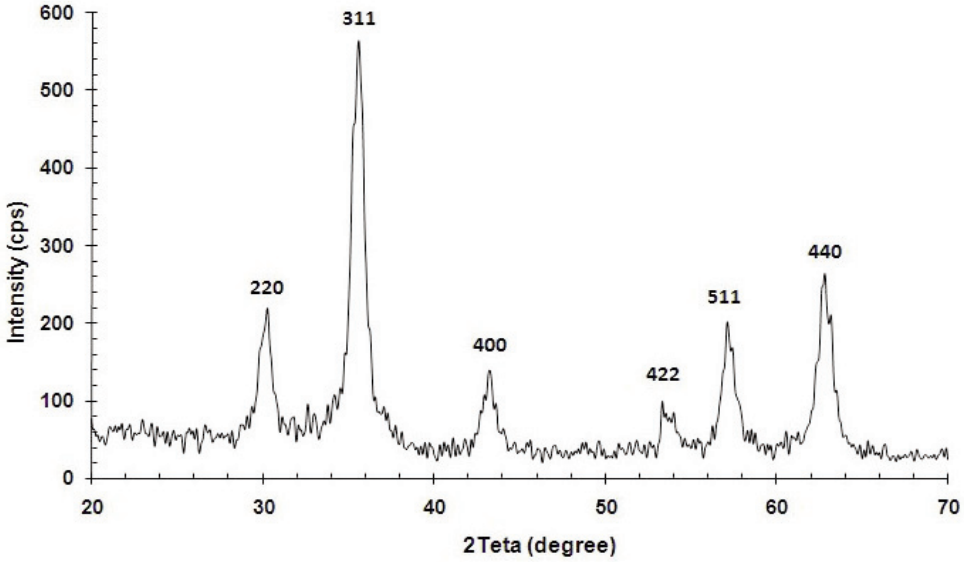

Fig.1. XRD pattern of the powder synthesized at 25^oC.

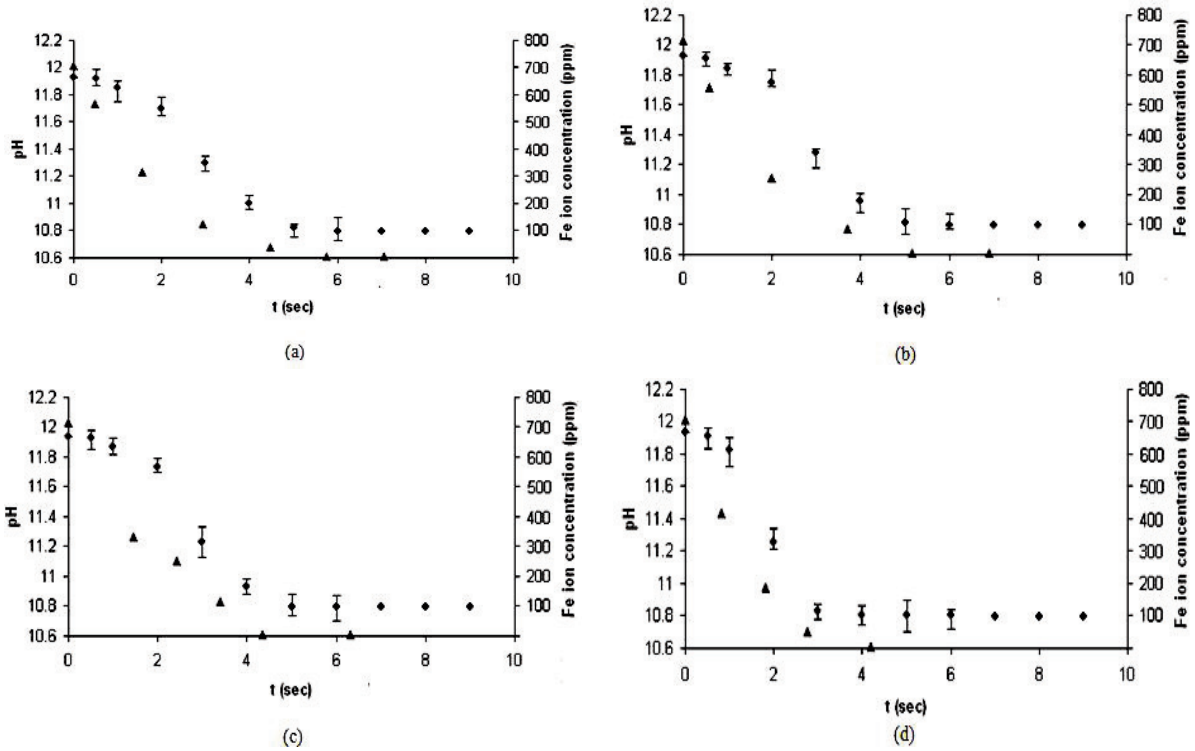

Fig.2. Variation in amount of pH (circles) and Fe concentration (triangles) of solution phase with time at a) 25 °C, b) 40 °C, c) 60 °C and 70 °C.

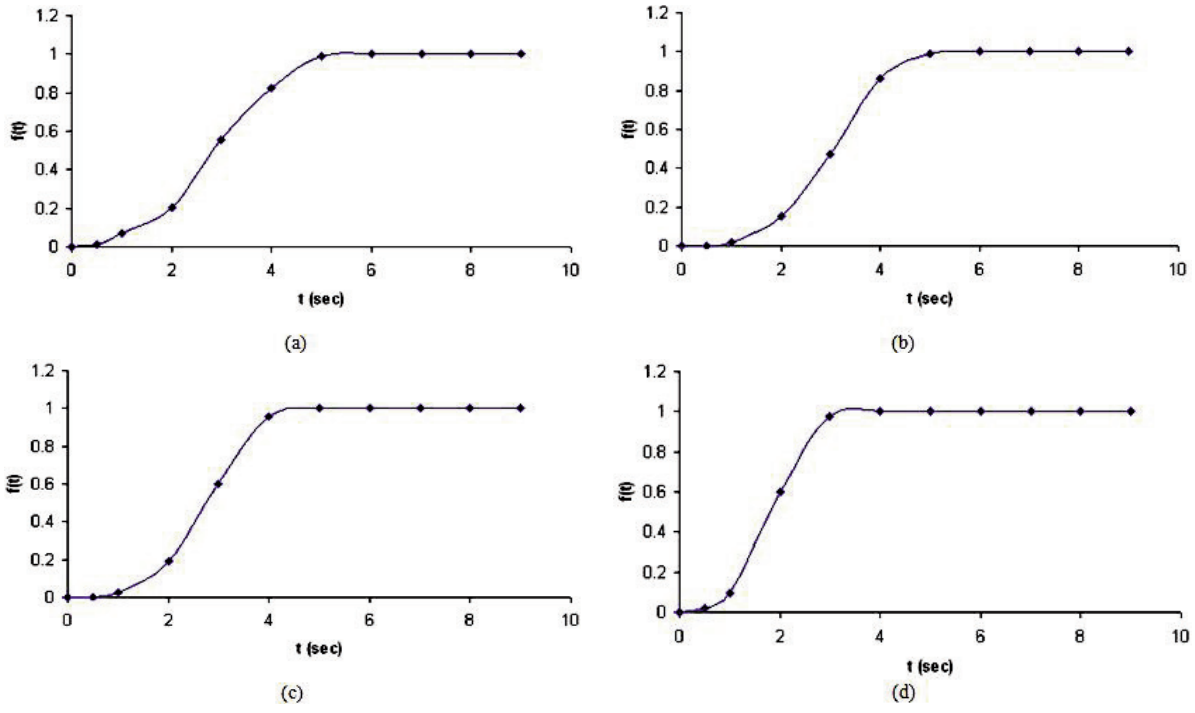

Fig.3. Fraction of reaction progression with time at a) 25 °C, b) 40 °C, c) 60 °C and 70 °C.

respectively. $\ln[-\ln(1-f(t))]-\ln t$ curves have been plotted at various temperatures in Fig. 4.

According to Fig. 2, in each temperature after at most 4 to 5 sec, pH variations reduce to negligible amounts and finally pH reaches a constant number. Some simple calculations will lead to *n* and *k* evaluation. Thus, the related *f(t)* functions for various temperatures can be written as:

$$f_{298}(t)=1-\exp(-0.031t^{3.08}) \quad ...(9)$$

$$f_{313}(t)=1-\exp(-0.048t^{3.04}) \quad ...(10)$$

$$f_{333}(t)=1-\exp(-0.08t^{2.93}) \quad ...(11)$$

$$f_{343}(t)=1-\exp(-0.13t^{2.92}) \quad ...(12)$$

As n is near 3 in equations (9) to (12), final semi-spherical shape of particles is expected. This result is in good agreement with TEM images of dried powders. According to Fig. 5, final mean diameter of nanoparticles produced at 25°C is about 24 nm. On the other hand, synthesis process is completed in about 4 sec according to pH and iron ion (concentration) measurements. Thus, mean linear growth rate *v* is about $3\ \frac{nm}{\sec}$. With this estimation, number of nucleation points *N* is about $2.65\times10^{23}\ \frac{nuclei}{m^3}$ from equation (3) which is logical for homogenous nucleation of initial nucleus. These amounts of *k*, *n*, *v* and *N* are dependent to environmental parameters such as temperature, initial pH, concentration of reactants, etc. However, general Avrami behavior of magnetite nanoparticles formation can be used for controlling the reaction progress.

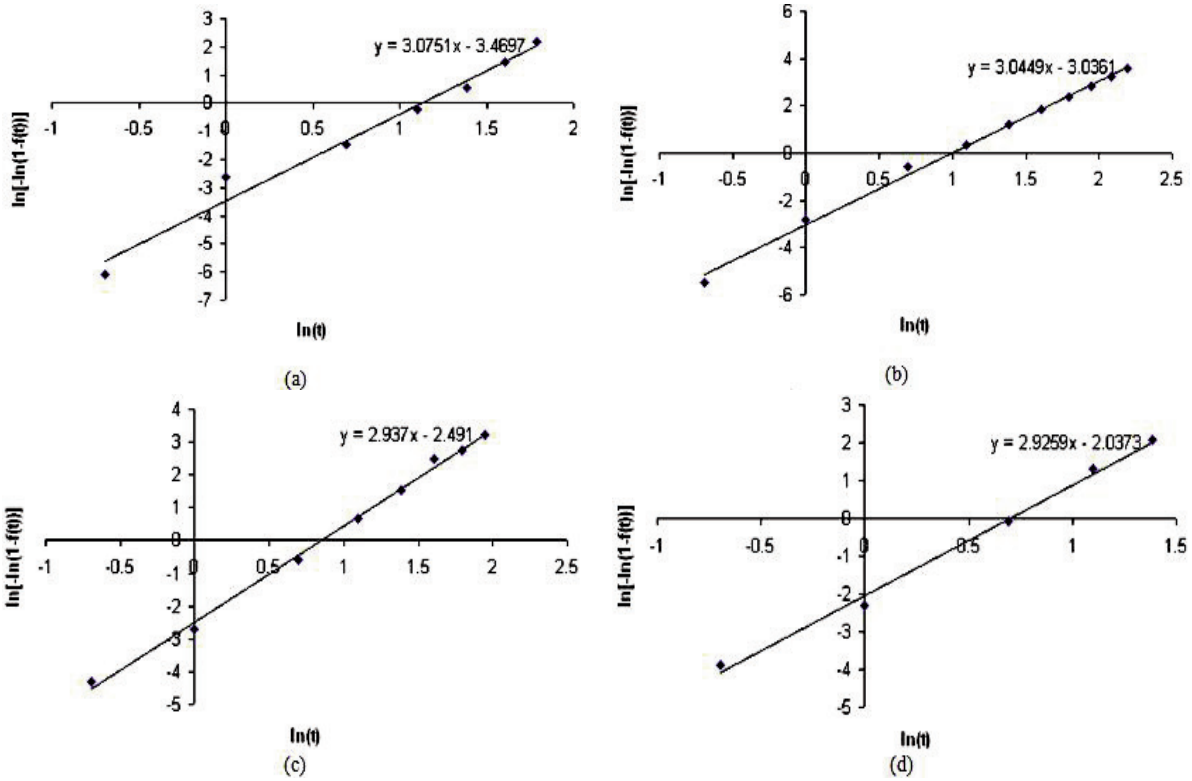

Fig. 4. $\ln[-\ln(1-f(t))]$ *vs.ln t curves at a) 25 °C, b) 40 °C, c) 60 °C and 70 °C.*

$t_{0.5}$ amounts at various temperatures are calculated from equations (9) to (12) and listed in table 1. $t_{0.5}$ is decreased with increase in temperature as seen in this table. $\ln t_{0.5} - \frac{1}{T}$ plot is shown in figure 6. $\frac{Q_E}{R}$ is equals to 885.85 using this diagram. These calculations are performed for various initial pHs and results are summarized in table 2.

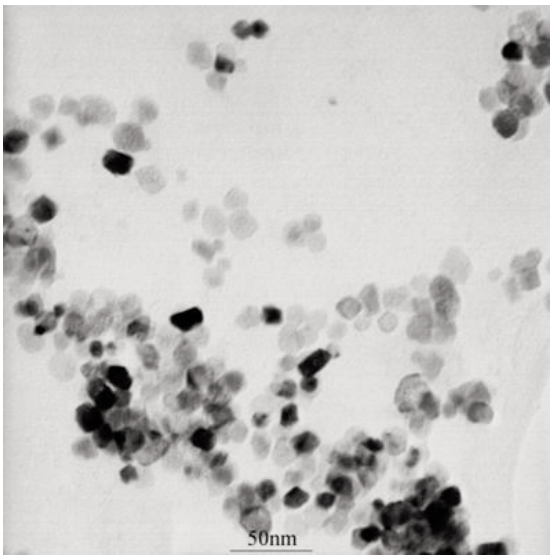

Fig. 5. TEM image of nanoparticles synthesize at 25 °C.

Table 1. Amounts of $t_{0.5}$ at various temperatures for initial pH=11.92

Temperature (°K)	298	313	333	343
$t_{0.5}$ (sec)	2.74	2.37	2.06	1.822

Table 2. Amounts of $\frac{Q_E}{R}$ measured at various initial pHs

pH	11.92	12.1	12.3
Q_E/R	885	905	950

4. Conclusion

Magnetite nanoparticles formation via co-precipitation method can reveal Avrami behavior by general equation of $f(t) = 1 - \exp(kt^n)$ k and n are functions of environmental parameters such as temperature, pH, concentration, stirring conditions, etc. According to presented data, $t_{0.5}$ is diminished with increase in temperature. On the other hand, driving force is increased with pH. Current efforts in our research group are attempting to demonstrate k and n

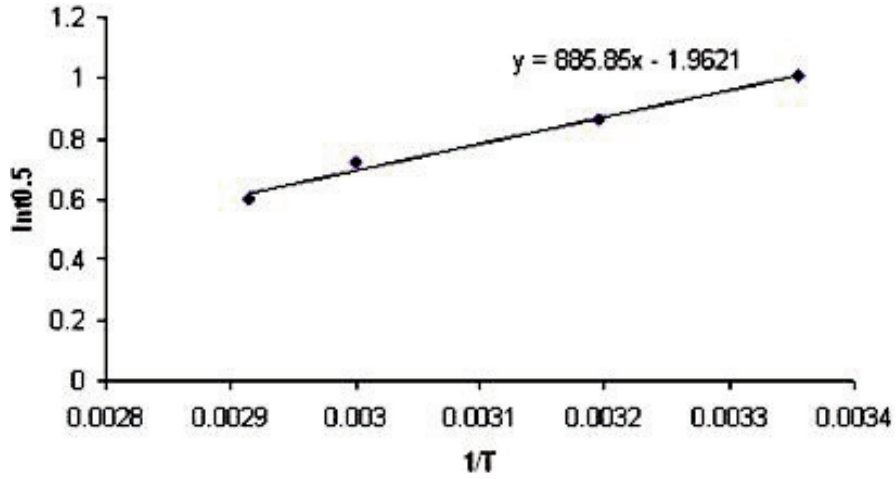

Fig. 6. $\ln t_{0.5} - \frac{1}{T}$ plot for reaction (1).

as functions of mentioned experimental parameters.

References

[1] S.C. Vanithakumari and K.K. Nanda, Phys. Lett. A, 372 (2008) 6930.

[2] G. Guisbiers and L. Buchaillot, Phys. Lett. A, 374 (2009) 305.

[3] E. Darezereshki and F. Bakhtiari, J. Min. Metall. Sect. B-Metall., 47 (2011) 73.

[4] L. LaConte, N. Nitin and G. Bao, Materials Today, 8 (2005) 32.

[5] M. Arruebo, R.F. Pacheco, M.R. Ibarra and J. Santamaria, Nanotoday, 2 (2007) 22.

[6] D.K. Kim, Y. Zhang, J. Kehr, T. Klason, B. Bjelke and M. Muhammed, J. Magen. Magen. Mater., 225 (2001) 256.

[7] K.L. Ang, S. Venkatraman and R.V. Ramanujan, Mater. Sci. Eng. C, 27 (2007) 347.

[8] C. Gruttner, K. Muller, J. Teller, F. Westphal, A. Foreman and R. Ivkov, J. Magen. Magen. Mater., 311 (2007) 181.

[9] C. Y. Wang, J. M. Hong, G. Chen, Y. Zhang and N. Gu, Chinese Chem. Lett., 21 (2010) 179.

[10] R. Mo, J. Yang, X.Wu and S. Lin, J. Magen. Magen. Mater., 323 (2011) 2287.

[11] A. Simchi, R. Ahmadi, S. M. Seyed Reihani and A. Mahdavi, Mater. and Des., 28 (2007) 850.

[12] R.Y. Hong, T.T. Pan, Y.P. Han, H.Z. Lib, J. Ding and S. Han, J. Magen. Magen. Mater., 310 (2007) 37.

[13] D. A. Porter and K. E. Easterling, “Phase Transformations in Metals and Alloys”, CRC Press, New York, 1992, p. 290.

[14] J. Malek and T. Mitsuhashi, J. Am. Ceram. Soc., 83 (2000) 2103.

[15] I. Haranczyk, B.Szafirska and K.Fitzner, J. Min. Metall. Sect. B-Metall., 38 (2002) 33.

[16] I. Nedkov, T. Merodiiska, L. Slavov, R.E. Vandenberghe, Y. Kusano and J. Takada, J. Magen. Magen. Mater., 300 (2006) 358.

[17] N. Gokon, A. Shimada, H. Kaneko, Y. Tamaura, K. Ito and T. Ohara, J. Magen. Magen. Mater., 238 (2002) 47.